

A Hybrid Early-Exit Algorithm for Large Language Models Based on Space Alignment Decoding (SPADE)

Bowen Zheng^{1,*}, Ming Ma^{1,2,*}, Zhongqiao Lin¹, Tianming Yang^{1,†}

¹Institute of Neuroscience, Key Laboratory of Brain Cognition and Brain-inspired Intelligence Technology, Center for Excellence in Brain Science and Intelligence Technology, Chinese Academy of Sciences, Shanghai, China
²University of Chinese Academy of Sciences
{zhengbw, mam2022, zqlin, tyang}@ion.ac.cn

*These authors contributed equally to this work. †Corresponding author

Abstract

Large language models are computationally expensive due to their deep structures. Prior research has shown that intermediate layers contain sufficient information to generate accurate answers, leading to the development of early-exit algorithms that reduce inference costs by terminating computation at earlier layers. However, these methods often suffer from poor performance due to misalignment between intermediate and output layer representations that lead to decoding inaccuracy. To address these challenges, we propose SPADE (SPace ALIGNment DEcoding), a novel decoding method that aligns intermediate layer representations with the output layer by propagating a minimally reduced sequence consisting of only the start token and the answer token. We further optimize the early-exit decision-making process by training a linear approximation of SPADE that computes entropy-based confidence metrics. Putting them together, we create a hybrid early-exit algorithm that monitors confidence levels and stops inference at intermediate layers while using SPADE to generate high-quality outputs. This approach significantly reduces inference costs without compromising accuracy, offering a scalable and efficient solution for deploying large language models in real-world applications.

1 Introduction

Large language models (LLMs) are deep. For instance, currently the largest LLaMA model reaches an impressive depth of 80 layers (Touvron et al., 2023), which incurs a significant inference cost. However, previous studies have shown that the information contained in the intermediate layers can be extracted to generate correct answers (nostalgia, 2020; Dar et al., 2023; Geva et al., 2023; Hendel et al., 2023; Belrose et al., 2023; Ghandeharioun et al., 2024). Based on these findings, a variety of early-exit algorithms has been proposed

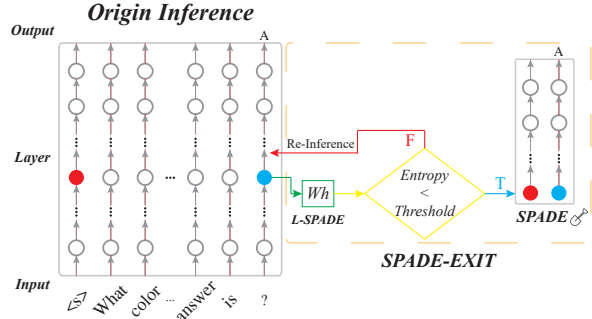


Figure 1: SPADE-EXIT algorithm. It contains a confidence-based decision-making mechanism to stop inference at an early layer. Then, SPADE, which propagates the rest of LLM with the start token and the answer token only, is used to generate answers. The confidence is evaluated with L-SPADE, which is a linear approximation of SPADE.

to speed up the inference by stopping at an early layer and generate answers based on the information contained in the early layer (Schuster et al., 2022; Pal et al., 2023; Din et al., 2024; Valade, 2024; Elhoushi et al., 2024; Fan et al., 2024; Zhang et al., 2024a).

The success of early-exit algorithms depend on the accuracy of decoding early layers. The most straightforward approach to decode from early layers is to apply the linear transformation matrix used for the final output layer to map intermediate layers directly to the vocabulary space, a technique known as Logit Lens (nostalgia, 2020). However, this method often fails, most likely due a misalignment between the intermediate layer's and the final layer's representational spaces (Ghandeharioun et al., 2024). More refined approaches such as Tuned Lens added a linear transformation to decode the intermediate layers and enhance the performance (Belrose et al., 2023). This linear transformation is trained to align the intermediate layers' outputs to match the outputs of the original LLM.

However, these linear decoding methods ignore the processing in later layers that cannot be captured by simple linear transformations, leading to their sub-optimal performance. This further limits the performance of early-exit algorithms built on these methods.

To address this issue, we develop a novel decoding method, termed SSpace Alignment DEcoding (SPADE), which does not rely on linear transformations. It propagate through the later layers with a minimally reduced sequence with two tokens — the start token and the answer token . This approach greatly reduces the computational cost, while providing a significant performance advantage over linear decoding methods.

Furthermore, to build an efficient early-exiting decision mechanism, we train a linear decoder, termed L-SPADE, to approximate SPADE, and use it to compute a entropy-based confidence metrics. L-SPADE achieves similar performance as SPADE in many cases. It provides good approximation without having to propagate through the later layers, further reducing the computational cost. Importantly, the linear transformation in L-SPADE trained on one dataset can be generalized to other datasets, further reducing the training cost.

Combining SPADE and L-SPADE, we propose SPADE-EXIT, an early-exit mechanism to accelerate LLM inference. By monitoring confidence levels at intermediate layers with L-SPADE, the method stops the inference process and uses SPADE to produce accurate results. With this hybrid mechanism, we reduce the number of forward propagation layers significantly without compromising answer quality.

In conclusion, SPADE-EXIT combines the novel SPADE decoding method and the efficient L-SPADE confidence estimator to significantly reduce inference costs for LLM without compromising accuracy. This approach offers a practical, scalable solution for leveraging intermediate layer information, enabling faster and more efficient deployment of LLMs.

2 Related Work

Hidden Representation Decoding A growing body of work shows that intermediate layers encode task-relevant semantics (Hendel et al., 2023; Wang et al., 2023; Halawi et al., 2024; Din et al., 2024). Logit Lens reuses the output embedding to map each hidden state to logits (nostalgia

2020), while Tuned Lens (Belrose et al., 2023) and Future Lens (Pal et al., 2023) use an extra linear mapping; PatchScope adopts a training-free variant (Ghandeharioun et al., 2024). Patching studies replace or ablate subsets of activations to test functional necessity, revealing that many tasks survive with most sequential context removed when intervention occurs in middle layers (Hendel et al., 2023; Wang et al., 2023; Pal et al., 2023; Zheng et al., 2024).

Prior decoders rely on linear mappings or external training signals. By contrast, we exploit the model’s own computation: we propagate a maximally reduced sequence that naturally aligns an early layer’s space to the output layer’s space, enabling accurate, early read out without auxiliary training.

Early Exit Scaling LLMs inflates inference cost, motivating efficiency techniques such as quantization (Zhang et al., 2024b; Hu et al., 2024; Hasan, 2024), pruning (Li et al., 2024; Fang et al., 2024), distillation (Wang et al., 2024; Ko et al., 2024; Di Palo et al., 2024), and early-exit ((Schuster et al., 2022; Pal et al., 2023; Din et al., 2024; Valade, 2024; Elhoushi et al., 2024; Fan et al., 2024; Zhang et al., 2024a)).

Among these methods, early-exit methods accelerate inference by terminating computation once a confidence threshold is met, either through threshold optimization (Zhang et al., 2024a; Fan et al., 2024) or architectural designs (Pal et al., 2023; Din et al., 2024; Valade, 2024) that support intermediate predictions.

We propose a hybrid early-exit mechanism. It uses linear mappings as fast confidence estimators and uses a more accurate reduced-sequence propagation mechanism to generate accurate answers.

3 Methods

The results presented in the main text is based on LLaMA-7b (Touvron et al., 2023) in the main text. Testing with additional models are included in Supplemetary. The datasets used include ARC (Clark et al., 2018), BoolQ (Clark et al., 2019), HeadQA (Vilares and Gómez-Rodríguez, 2019), and Wikitext-103 (Merity et al., 2016).

Following the definition of auto-regressive transformer (Vaswani et al., 2017), a decoder-only large language model \mathcal{M} , such as Llama (Touvron et al., 2023), consists of multiple transformer blocks, where each block corresponds to a layer

$l \in [1, 2, \dots, L]$. Given an input sequence $S = \{x_1, x_2, \dots, x_n\}$, where x_i represents the i -th token in the sequence. The tokens are embedded with the embedding function:

$$e_i = E(x_i) \quad (1)$$

where E is the embedding layer that maps tokens to a continuous vector space. The embedding matrix is denoted as $E \in \mathbb{R}^{V \times d}$, where V is the vocabulary size and d is the embedding dimension.

The hidden representation of the i -th token at layer l is denoted as h_i^l . It is computed iteratively through each transformer block, where each layer l applies a transformation T to the output from the previous layer:

$$h_i^l = T(h_i^{l-1}). \quad (2)$$

T consists of multi-head self-attention and feedforward layers. By convention, the embedding layer is considered as layer 0, i.e.,

$$h_i^0 = e_i \quad (3)$$

At the final layer L , a linear transformation projects the hidden state onto a logits space of vocabulary size V :

$$z_i^L = Wh_i^L \quad (4)$$

where $W \in \mathbb{R}^{V \times d}$ are the learnable parameters of the linear layer. Finally, a softmax function is applied to obtain the probability distribution over the vocabulary:

$$p_i^i = \text{softmax}(z_i) \quad (5)$$

where $p_i \in \mathbb{R}^V$ represents the probability distribution of the next token at position i .

4 Motivation

Although methods such as Logit Lens (nostalgabrainst, 2020) may extract answer information from early layers, there is a mismatch between their performance and the actual information contained in the early layers. For example, when tested on Llama-7b with ARC dataset, the answer information is contained in layers as early as layer 15, where PCA reveals clear clustering patterns and decision boundaries in a linear space (Figure 2a). A linear classifier trained on the principal components derived from the intermediate layer's hidden states significantly outperforms Logit Lens in early layers (Figure 2b). The results suggest that these methods fail to appropriately extract the information from early layers.

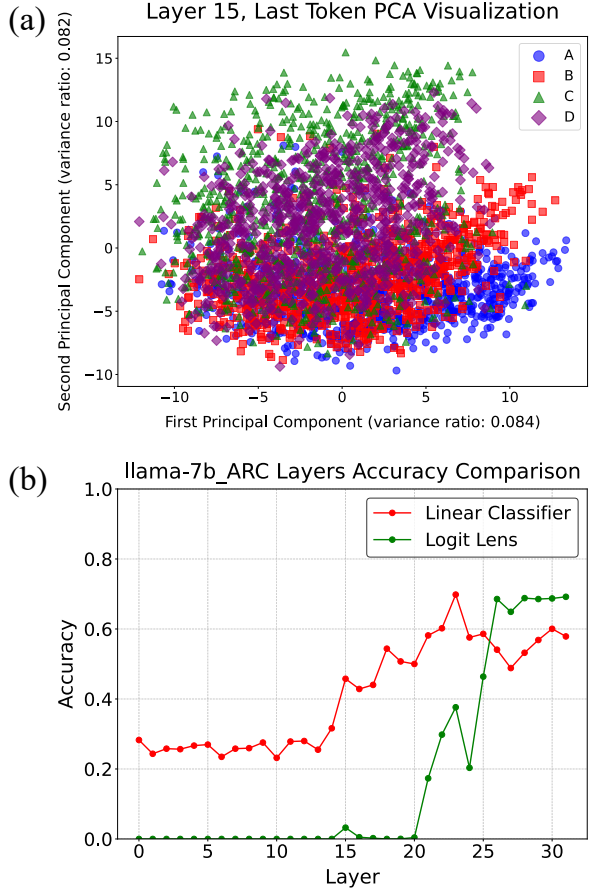


Figure 2: (a) PCA visualization of hidden states at the last token position (layer 15, ARC dataset). Clear clustering of answer choices (A-D) emerges, indicating early-layer answer representation. (b) Classification accuracy of a linear classifier trained on PCA-reduced hidden states from intermediate layers (ARC dataset). The classifier significantly outperforms Logit Lens in extracting answer information from early layers.

5 SSpace Alignment DEcoding (SPADE)

Here, we propose the SSpace Alignment DEcoding (SPADE) method, which takes advantage of the forwarding process of the original LLM to decode the information from early layers.

For a given intermediate layer l , we construct a minimal sequence that consists of only the start token, commonly denoted as $\langle s \rangle$, and the final answer token $\langle a \rangle$ of the original sequence. Both the start token and the final answer token contains minimal information from the complete sequence. Thereby, the additional processing in the later layers can be limited to representational space shift.

Subsequently, we forward this sequence from the l -th layer to the final layer L , obtaining:

$$[\langle s \rangle^L, \langle a \rangle^L] = T_l^L([\langle s \rangle^l, \langle a \rangle^l]) \quad (6)$$

where T_l^L denotes the transformation after forward-ing the selected tokens through the transformer model from the l -th layer to the final layer L , and $\langle s \rangle^L, \langle a \rangle^L$ are the transformation output. With Eq. (4) and (5), we further obtain the probability distribution of the answer token $\langle a \rangle$ over the vocabulary space.

To evaluate the performance of SPADE, we plot the accuracy of SPADE applied to each intermediate layer and compare it against other methods (Figure 3). In the ARC dataset, the performance of the SPADE starts to rise above the baseline at layer 14 and reaches the naive LLM’s accuracy by layer 18. In comparison, Logit Lens has a lower baseline. Its performance only starts to rise above the baseline at layer 21 and stays below that of the SPADE until layer 28.

The start token $\langle s \rangle$ is crucial for SPADE’s performance. When it is removed, the performance in the ARC dataset is significantly impacted, reaching the naive LLM model’s accuracy only after layer 20. Notice that the baseline in this case is also lower than the SPADE and only comparable to Logit Lens, suggesting that the start token, widely used as a positional anchor in transformer models, contributes crucial task information that SPADE can utilize.

The same trend can be further validated in the BoolQ and HeadQA dataset (Figure 3), suggesting SPADE’s superior performance in general.

5.1 Linear-SPADE (L-SPADE): Approximation With Linear Projection

Adaptable early-exit algorithm requires the evalua-tion of early layers. Although SPADE propa-gates only two tokens, we hope that we can further reduce the computational cost of this evaluation by approximating SPADE with a learned linear mapping. The resulting linear mapping is termed Linear-SPADE (L-SPADE).

Specifically, for an early layer l ($0 < l \leq L$), our objective is to obtain a linear mapping that transforms representational space of layer l to that of layer L :

$$\hat{h}_i^L = \mathcal{F}(h_i^l) \quad (7)$$

where h_i^l is the hidden states in layer l , \mathcal{F} is the linear mapping function, and \hat{h}_i^L is the prediction produced with \mathcal{F} .

Distinct from methods such as Tuned Lens (Bel-rose et al., 2023), the target of training h_i^L is not the output of the original transformer model. Instead,

it is obtained from SPADE, as described in Eq. (6). \mathcal{F} is trained by minimizing the cross-entropy loss between the two logits z_i^L and \hat{z}_i^L computed from h_i^L and \hat{h}_i^L with Eq. (4):

$$\mathcal{L} = CE(z_i^L, \hat{z}_i^L) \quad (8)$$

where CE is the cross-entropy loss, defined as:

$$CE(p) = - \sum_i p_i \log(p_i)$$

This linear approximation process is essentially distillation. By using SPADE as the distillation tar-get, we focus solely on representational space shift and minimize the interference from the additional sequence processing in later layers.

5.2 Performance

We evaluate the performance of SPADE, L-SPADE, and Logit Lens on the ARC, BoolQ, and HeadQA datasets. As shown in Figure 3, SPADE and L-SPADE consistently outperforms Logit Lens significantly. Both methods start to generate results more accurate than the baseline earlier than Logic Lens and reaches the naive LLM performance in earlier layers.

We further investigate whether the L-SPADE mapping trained with a particular dataset can be generalized to other datasets. Here, we train the L-SPADE mappings on ARC datasets and evaluate them on the BoolQ, HeadQA, and Wikitext-103 dataset with the perplexity metrics. As shown in Figure 4, SPADE, which does not rely on training, achieves the lowest perplexity, outperforming the linear decoding methods, including Logit Lens, Tuned Lens, and L-SPADE across almost all layers. L-SPADE often achieves lower perplexity than Tuned Lens, especially on larger dataset such as Wikitext-103, demonstrating the advantage of us-ing SPADE as the target to train linear mappings. In addition, while the training of Tuned Lens requires the propagation of all tokens in the naive LLM, the training of L-SPADE uses only two tokens and substantially reduces the training cost.

Overall, these results indicate that SPADE can be used for accurate decoding of early-layer representations and its linear approximation, L-SPADE, can match or exceed the performance of Tuned Lens with far less training overhead.

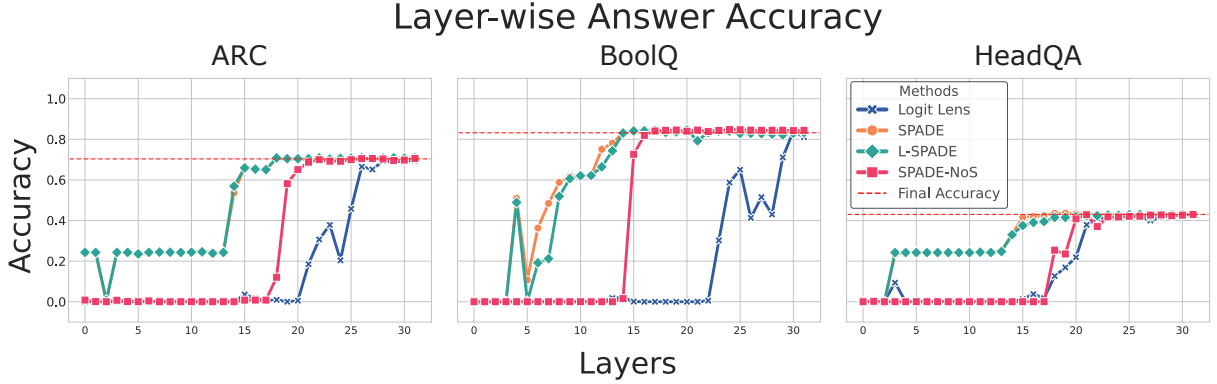


Figure 3: Layer-wise answer accuracy on the ARC (left), BoolQ (middle), and HeadQA (right) dataset for Logit Lens, SPADE, L-SPADE, and SPADE-NoS (SPADE without the start $\langle s \rangle$ token). The dashed line indicates the naive LLM model’s task accuracy. The SPADE variants outperform Logit Lens. Omitting the start token incurs a performance drop (pink trace).

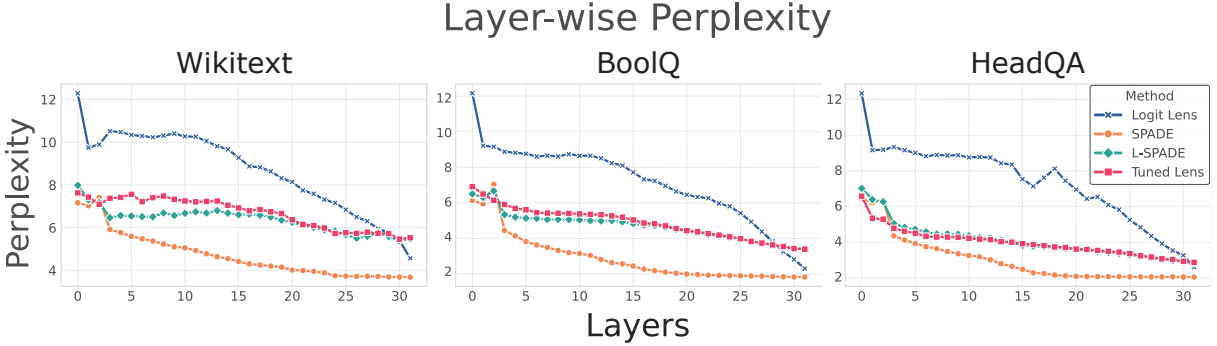


Figure 4: Layer-wise perplexity on WikiText-103 (left), BoolQ (middle) and HeadQA (right) dataset. Linear mappings used in L-SPADE and Tuned Lens are trained on ARC. Lower perplexity indicates better decoding performance.

6 SPADE-EXIT: Accelerating LLMs with SPADE

While L-SPADE provides fast decoding with a simple linear transformation, SPADE, due to its task-agnostic nature, still performs better, especially when tested across different tasks. Therefore, we combine the two to build SPADE-EXIT, a hybrid early-exit mechanism that takes advantage of both methods.

6.1 Entropy-Based Confidence Metrics with L-SPADE

First, we need to have a decision mechanism for early-exit. By adopting a suitable confidence metric, we may determine whether the model can produce reasonable outputs at an intermediate layer, thereby skipping the subsequent layers and improving its inference speed. As the confidence has to be evaluated for each layer before the exit, we adopt L-SPADE for its efficiency.

One of the most commonly used metrics for

making early-exit decisions is to compute the difference between the probabilities of the top two predicted tokens (Fan et al., 2024; Din et al., 2024). A larger difference indicates higher confidence in the model’s prediction. However, this probability-based metric is not ideal. When multiple tokens are similarly plausible, the model may be overly conservative, which reduces the efficiency of potential early exits (Schuster et al., 2022). To address this limitation, here, we employ an entropy-based metric in our method. We compute an entropy score for each candidate early-exit layer:

$$H^{(l)} = - \sum_{v=1}^V p_v^{(l)} \log p_v^{(l)}, \quad (9)$$

where $p^{(l)} \in \mathbb{R}^V$ is the L-SPADE soft-max distribution at layer l . Lower $H^{(l)}$ means the probability mass is more concentrated—i.e., higher confidence.

Algorithm 1 SPADE-EXIT

Require: Pre-trained L-SPADE, threshold T, evaluation interval N

```
1: for  $i$  from 0 to  $L$  do
2:   if  $trunc$  then
3:      $x_i = SPADE_i(x_{i-1})$ 
4:      $Cache_i = updateCache(x_i)$ 
5:   else
6:      $x_i = Layer_i(x_{i-1})$ 
7:   end if
8:   if  $i \bmod N = 0$  then
9:      $E_i = Entropy(SPADE_{linear}(x_i))$ 
10:    if  $E_i \leq T$  then
11:       $trunc = True$ 
12:    end if
13:   end if
14: end for
```

6.2 Adaptive Early-Exit Mechanism

Based on the entropy-based confidence metric, we establish an adaptive early-exit mechanism. When the confidence exceeds a predefined threshold, the inference process is terminated. Similar thresholding mechanism has been demonstrated in the brain (Gold and Shadlen, 2002; Gold and Shadlen, 2007; Kira et al., 2015). Adjusting threshold allows us to achieve a balance between accuracy and speed, which can be optimized for different application scenarios.

As we have demonstrated the performance advantage of SPADE, we use it to produce answers once the inference is stopped. The complete SPADE-EXIT algorithm is detailed in Algorithm 1, referred to as.

With the original LLM model, a full forward pass of a sequence of length n has the time complexity of $\mathcal{O}(n^2)$. SPACE-EXIT reduces the complexity from quadratic to linear $\mathcal{O}(1)$ once the metrics exceeds the predefined threshold, since we only need to forward two tokens.

6.3 Performance

Finally, we evaluate the performance of SPACE-EXIT on the ARC, BoolQ, and HeadQA datasets using the LLaMA model (Figure 5). Additional results for Vicuna are provided in Appendix B.1. The experiments demonstrate that our method is effective across diverse datasets, delivering results without significantly compromising accuracy. By adjusting the exit threshold, we can balance between accuracy and inference speed. With an appropri-

ately chosen threshold, the model is able to produce reasonable outputs from earlier layers without degrading performance. In addition, as the linear mappings used in L-SPADE are generalizable to different tasks, SPADE-EXIT trained in one task can also perform well in other tasks (Figure 6).

7 Discussion

Our results suggest that to extract answer information from the intermediate layers, we need to address two issues. First, we need to align the representational space of the intermediate layers to that of the final output layer for accurate decoding. This can be achieved with a linear mapping. Second, there is additional task-related processing in the later layers that cannot be captured by simple linear mappings. The SPADE method, which propagates the start token along with the answer token, is an effective way to address this issue.

In the future, we may train LLMs by restraining the representational space to be the same across all layers. Thereby, additional linear mappings will be no longer necessary for decoding early layers. Yet, the SPADE method should remain useful to generate more accurate answers.

8 Conclusion

In this work, we introduce SPADE decoding method, which decode answer information from intermediate layers without requiring additional training. Additionally, we develop L-SPADE, a lightweight and generalizable linear approximation of SPADE, to efficiently compute entropy-based confidence metrics for early-exit decisions.

Building on these methods, we develop SPADE-EXIT, a novel hybrid early-exit algorithm that significantly accelerates inference in LLMs while maintaining high accuracy. Our results demonstrate that SPADE-EXIT effectively reduces computational costs by enabling accurate predictions from intermediate layers, achieving competitive performance across diverse datasets and models. These advancements offer a powerful framework for efficiently deploying LLMs in real-world applications, balancing inference speed and performance without compromising output quality.

9 Limitation

Although our algorithm is suitable for multi-token tasks, our current experiments focus on single-token generation, and the extension of this ap-

SPADEF-EXIT Performance: Accuracy-Speed Trade-off

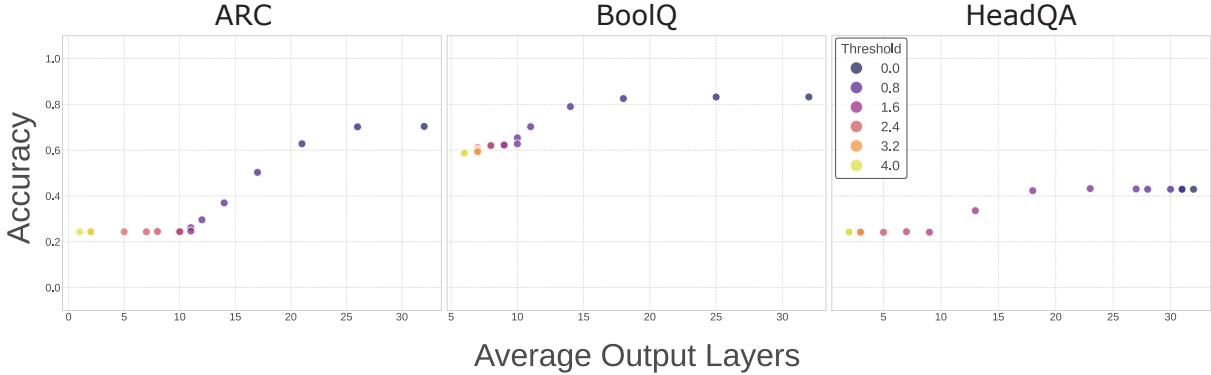


Figure 5: Performance of SPADEF-EXIT on the ARC (left), BoolQ (middle) and HeadQA (right) datasets. Adjusting the threshold (indicated with different colors) allows SPADEF-EXIT to balance inference speed and accuracy. Lower entropy thresholds result in later exits and higher accuracy, while higher thresholds yield earlier exits and faster inference with a trade-off in accuracy.

Generalization of SPADEF-EXIT

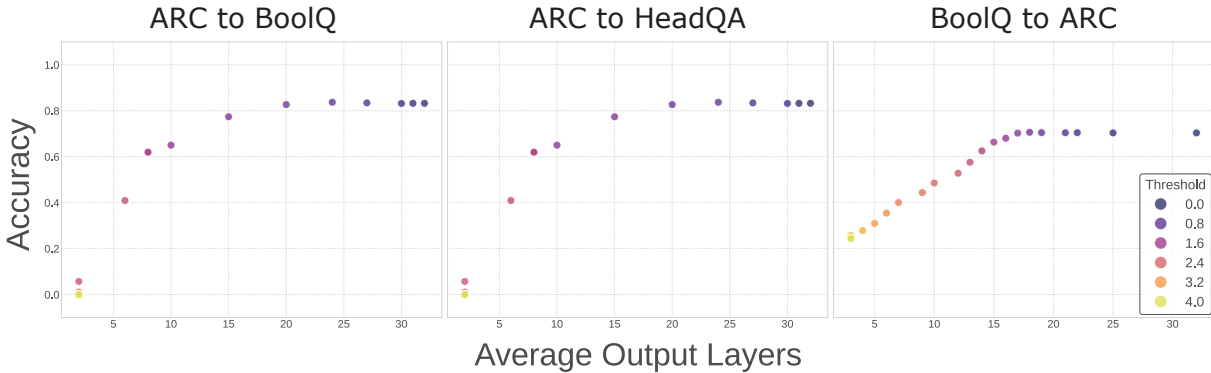


Figure 6: Performance of SPADEF-EXIT on BoolQ (left) and HeadQA (middle) datasets with L-SPADE trained on ARC and on ARC dataset with L-SPADE trained on BoolQ (right).

proach to multi-token outputs remains an open challenge. Additionally, while the method has been tested across multiple datasets and models, further exploration is needed to evaluate its performance on more diverse tasks and architectures.

answering? try arc, the ai2 reasoning challenge. *Preprint*, arXiv:1803.05457.

Guy Dar, Mor Geva, Ankit Gupta, and Jonathan Berant. 2023. [Analyzing transformers in embedding space](#). *Preprint*, arXiv:2209.02535.

Flavio Di Palo, Prateek Singh, and Bilal Fadlallah. 2024. Performance-guided llm knowledge distillation for efficient text classification at scale. *arXiv preprint arXiv:2411.05045*.

Alexander Yom Din, Taelin Karidi, Leshem Choshen, and Mor Geva. 2024. [Jump to conclusions: Shortcutting transformers with linear transformations](#). *Preprint*, arXiv:2303.09435.

Mostafa Elhoushi, Akshat Shrivastava, Diana Liskovich, Basil Hosmer, and Bram Wasti. 2024. [Layerskip: Enabling early exit inference and self-speculative decoding](#). In *Proceedings of the 62nd Annual Meeting of the Association for Computational Linguistics (Volume 1: Long Papers)*, pages 12622–12642.

- Siqi Fan, Xin Jiang, Xiang Li, Xuying Meng, and Peng Han. 2024. Not all layers of llms are necessary during inference. *Preprint*, arXiv:2403.02181.
- Gongfan Fang, Hongxu Yin, Saurav Muralidharan, Greg Heinrich, Jeff Pool, Jan Kautz, Pavlo Molchanov, and Xinchao Wang. 2024. Maskllm: Learnable semi-structured sparsity for large language models. *arXiv preprint arXiv:2409.17481*.
- Mor Geva, Jasmijn Bastings, Katja Filippova, and Amir Globerson. 2023. Dissecting recall of factual associations in auto-regressive language models. *Preprint*, arXiv:2304.14767.
- Asma Ghandeharioun, Avi Caciularu, Adam Pearce, Lucas Dixon, and Mor Geva. 2024. Patchscopes: A unifying framework for inspecting hidden representations of language models. *Preprint*, arXiv:2401.06102.
- Joshua I Gold and Michael N Shadlen. 2002. Banburismus and the brain: decoding the relationship between sensory stimuli, decisions, and reward. *Neuron*, 36(2):299–308.
- Joshua I Gold and Michael N Shadlen. 2007. The neural basis of decision making. *Annu. Rev. Neurosci.*, 30(1):535–574.
- Danny Halawi, Jean-Stanislas Denain, and Jacob Steinhardt. 2024. Overthinking the truth: Understanding how language models process false demonstrations. *Preprint*, arXiv:2307.09476.
- Jahid Hasan. 2024. Optimizing large language models through quantization: A comparative analysis of ptq and qat techniques. *arXiv preprint arXiv:2411.06084*.
- Roei Hendel, Mor Geva, and Amir Globerson. 2023. In-context learning creates task vectors. *Preprint*, arXiv:2310.15916.
- Xing Hu, Yuan Cheng, Dawei Yang, Zhihang Yuan, Jiayong Yu, Chen Xu, and Sifan Zhou. 2024. I-llm: Efficient integer-only inference for fully-quantized low-bit large language models. *arXiv preprint arXiv:2405.17849*.
- Shinichiro Kira, Tianming Yang, and Michael N Shadlen. 2015. A neural implementation of wald’s sequential probability ratio test. *Neuron*, 85(4):861–873.
- Jongwoo Ko, Sungnyun Kim, Tianyi Chen, and Se-Young Yun. 2024. Distillm: Towards streamlined distillation for large language models. *arXiv preprint arXiv:2402.03898*.
- Jianwei Li, Yijun Dong, and Qi Lei. 2024. Greedy output approximation: Towards efficient structured pruning for llms without retraining. *arXiv preprint arXiv:2407.19126*.
- Stephen Merity, Caiming Xiong, James Bradbury, and Richard Socher. 2016. Pointer sentinel mixture models. *arXiv preprint arXiv:1609.07843*.
- nostalgebraist. 2020. Interpreting gpt: The logit lens. LessWrong blog post.
- Koyena Pal, Jiuding Sun, Andrew Yuan, Byron C. Wallace, and David Bau. 2023. Future lens: Anticipating subsequent tokens from a single hidden state. In *Proceedings of the 27th Conference on Computational Natural Language Learning (CoNLL)*, pages 548–560.
- Tal Schuster, Adam Fisch, Jai Gupta, Mostafa Dehghani, and Dara Bahri. 2022. Confident adaptive language modeling. *Preprint*, arXiv:2207.07061.
- Hugo Touvron, Thibaut Lavril, Gautier Izacard, Xavier Martinet, and Marie-Anne Lachaux. 2023. Llama: Open and efficient foundation language models. *Preprint*, arXiv:2302.13971.
- Florian Valade. 2024. Accelerating large language model inference with self-supervised early exits. *Preprint*, arXiv:2407.21082.
- Ashish Vaswani, Noam Shazeer, Niki Parmar, Jakob Uszkoreit, Llion Jones, Aidan N Gomez, Łukasz Kaiser, and Illia Polosukhin. 2017. Attention is all you need. *Advances in neural information processing systems*, 30.
- David Vilares and Carlos Gómez-Rodríguez. 2019. Head-qa: A healthcare dataset for complex reasoning. *Preprint*, arXiv:1906.04701.
- Lean Wang, Lei Li, Damai Dai, Deli Chen, and Hao Zhou. 2023. Label words are anchors: An information flow perspective for understanding in-context learning. *Preprint*, arXiv:2305.14160.
- Shuo Wang, Chihang Wang, Jia Gao, Zhen Qi, Hongye Zheng, and Xiaoxuan Liao. 2024. Feature alignment-based knowledge distillation for efficient compression of large language models. *arXiv preprint arXiv:2412.19449*.
- Jun Zhang, Jue Wang, Huan Li, Lidan Shou, and Ke Chen. 2024a. Draft & verify: Lossless large language model acceleration via self-speculative decoding. In *Proceedings of the 62nd Annual Meeting of the Association for Computational Linguistics (Volume 1: Long Papers)*, pages 11263–11282.
- Yi Zhang, Fei Yang, Shuang Peng, Fangyu Wang, and Aimin Pan. 2024b. Flattenquant: Breaking through the inference compute-bound for large language models with per-tensor quantization. *arXiv preprint arXiv:2402.17985*.
- Bowen Zheng, Ming Ma, Zhongqiao Lin, and Tianming Yang. 2024. Distributed rule vectors is a key mechanism in large language models’ in-context learning. *arXiv preprint arXiv:2406.16007*.

A Supplementary Experiments for SPADE

This appendix complements Section 5 by presenting SPADE and L-SPADE results on the Vicuna-7B model. All hyperparameters and evaluation protocols strictly follow those used for LLaMA-7B in the main text.

Figure 7 shows the performance of SPADE-based decoding for Vicuna-7B on the ARC, BoolQ, and HeadQA datasets, respectively. Across all three tasks, Vicuna-7B exhibits similar trends to those observed in LLaMA-7B. Both SPADE and L-SPADE significantly outperform Logit Lens and removing the start token leads to significantly poorer performance. These results confirm the SPADE’s effectiveness in instruction-tuned variants like Vicuna.

When using LLaMA and Vicuna models, we first perform LoRA-based fine-tuning on the downstream datasets to ensure good performance. We also evaluate their performance without fine-tuning. Although the overall perplexity is higher without fine-tuning, the SPADE method still demonstrated a significant advantage over other approaches as shown in Figure 8.

B Supplementary Experiments for SPADE-EXIT

B.1 Additional Performance on Other Datasets and Models

This appendix complements the performance results in Section 6. SPADE-EXIT based on two models (LLaMA-7B and Vicuna-7B) are tested across all three datasets (ARC, BoolQ, and HeadQA). All experiments use the same adaptive thresholding setup as described in the main text.

Figure 9 shows that SPADE-EXIT consistently achieves competitive accuracy while enabling early termination across layers. These results confirm the general effectiveness of SPADE-EXIT in a variety of QA tasks and models.

B.2 Additional Generalization Performance on Other Datasets and Models

This section expands on the generalization analysis, presenting full results where SPADE-EXIT is applied to unseen datasets using L-SPADE mappings trained on other datasets. Results are shown for both LLaMA-7B and Vicuna-7B across all dataset permutations (ARC, BoolQ, HeadQA).

The performance curves in Figures 10 and 11 demonstrate that SPADE-EXIT generalizes well across different tasks.

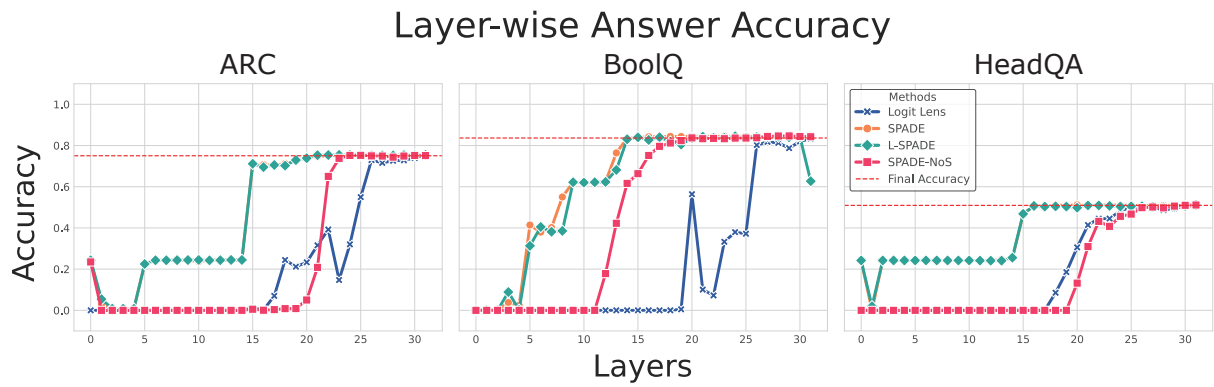


Figure 7: SPADE performance by Vicuna.

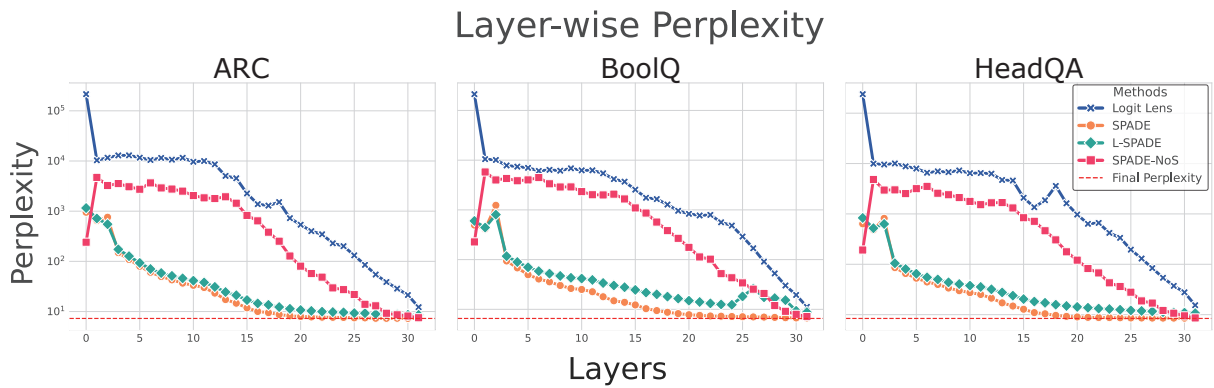


Figure 8: The perplexity with vanilla llama model with different methods.

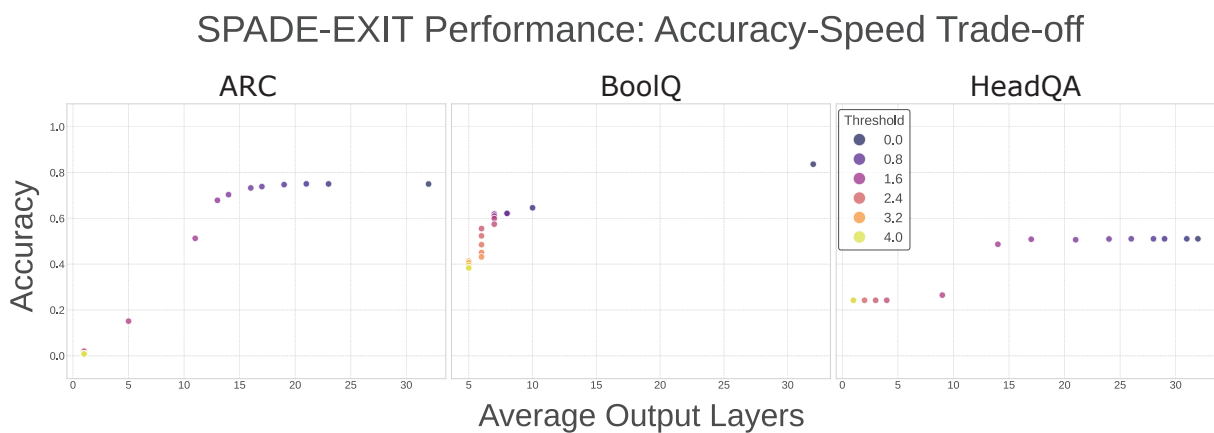


Figure 9: Performance of SPADE-EXIT by Vicuna.

Generalization of SPADE-EXIT

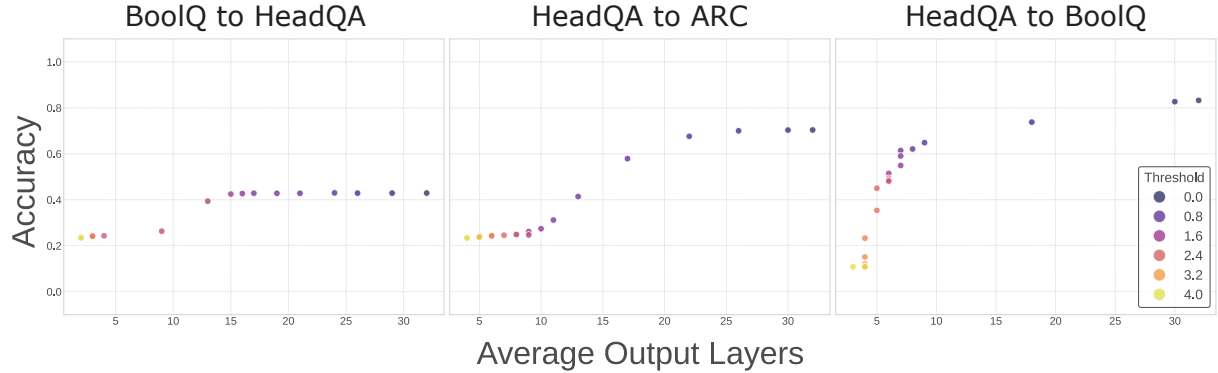


Figure 10: SPADE-EXIT performance of SPADE-EXIT with L-SPADE . (Llama-7b)

Generalization of SPADE-EXIT

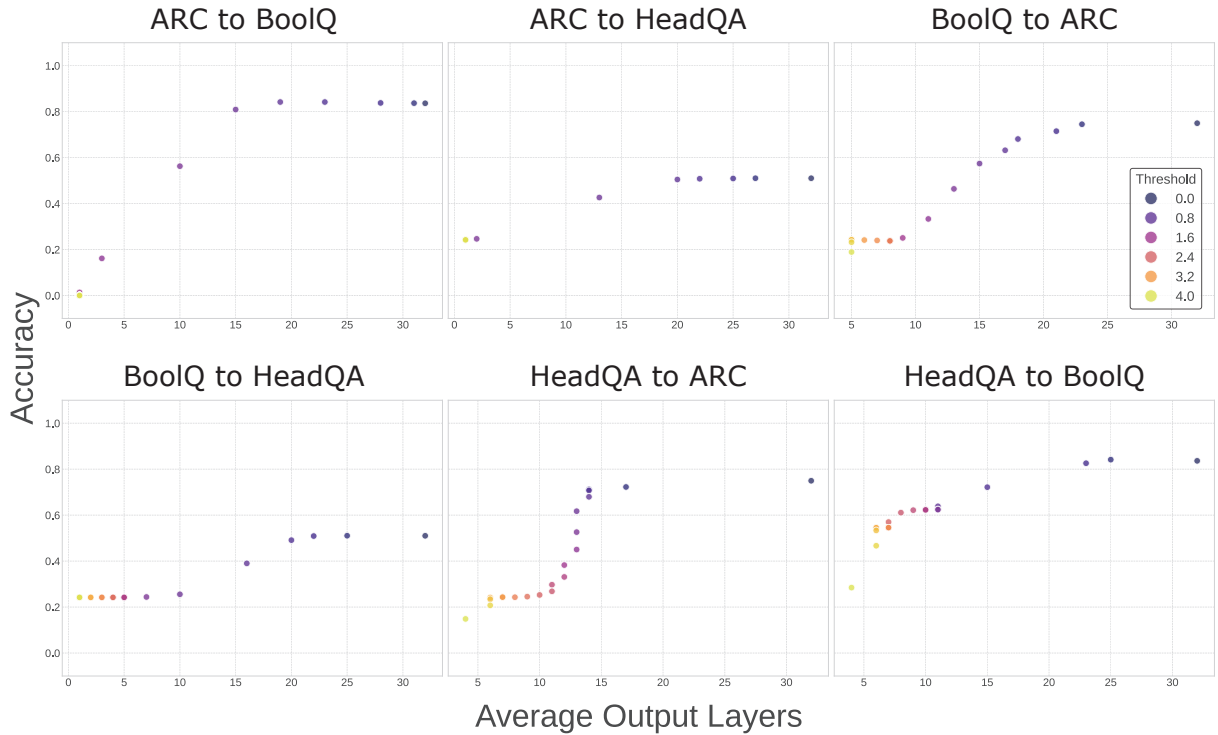


Figure 11: SPADE-EXIT performance of SPADE-EXIT with L-SPADE. (Vicuna-7b)